Presented at the Sixth Annual Workshop on
Geothermal Reservoir Engineering, Stanford
Geothermal Program, Stanford University,
Stanford, CA, December 16-18, 1980

A NUMERICAL SIMULATION OF THE NATURAL EVOLUTION OF VAPOR-DOMINATED HYDROTHERMAL SYSTEMS

K. Pruess and A.H. Truesdell

December 1980

Prepared for the U.S. Department of Energy
under Contract W-7405-ENG-48

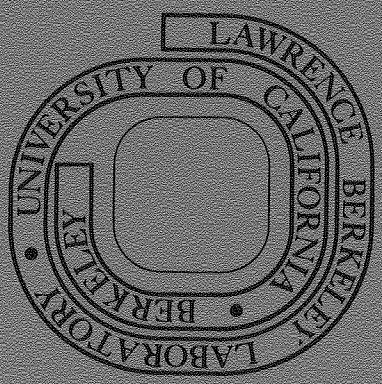

DISCLAIMER

LBL-12039

A Numerical Simulation of the Natural Evolution of Vapor-Dominated Hydrothermal Systems

by K. Pruess

Lawrence Berkeley Laboratory
University of California
Berkeley, California 94720

and

A. H. Truesdell

U.S. Geological Survey
Menlo Park, California 94025

This work was supported by the Assistant Secretary for Resource Applications, Office of Industrial and Utility Applications and Operations, Geothermal Energy Division of the U. S. Department of Energy under Contract W-7405-ENG-48.

Introduction

The natural state and the evolution of vapor-dominated hydrothermal systems have been the subject of considerable research and controversy (see References 1-4, and references therein). White, Muffler, and Truesdell have formulated a comprehensive qualitative model of vapor-dominated reservoirs.[3] Their work forms the basis for more recent attempts to understand reservoir processes in more quantitative detail.[5]

Most previous computational studies of natural fluid and heat flow in geothermal reservoirs have attempted to model specific reservoirs or have investigated more generalized steady-state convection in single-phase fluid (Ref. 6 and references therein) or in two-phase fluid.[7,8] In contrast, we describe simulation of the transient evolution of a "cold" hydrothermal system into a steady-state partially vapor-dominated system.

In our study we have neglected the effects of salts and gases and have assumed that rock properties are time independent and homogeneous within each part of the system. Despite these simplifications we believe that our model demonstrates the essential features of a natural hydrothermal convection system (NHCS).

Parameters of the System

The model system consists of a main permeable reservoir of water-saturated porous rock, overlain by a cap of less permeable rock (Figure 1). Through the caprock, the reservoir communicates with surface waters of ambient conditions (discharge and recharge). Also, conductive heat flow can occur across the caprock. The system is driven by a powerful heat source at its base.

A system of this type has a long transient period. Very large amounts of fluid must flow before convection patterns evolve into a steady state. Several thousand time steps are required for a computer simulation of this process. In order to make the computation economically feasible, a prudent design of system geometry and spatial discretization is required. We model a system with cylindrical symmetry, which allows us to employ a two-dimensional grid (Figure 2). The most critical element in the simulation is vertical pressure resolution. A coarse discretization in the vertical direction would average pressures and thereby inhibit onset and spreading of boiling. Finer gridding introduces more and smaller elements, which increases the computational work per time step and, moreover, reduces time step sizes due to throughput limitations. While our test calculations showed that a vertical grid spacing of 100 m or less is desirable, we had to use a compromise value of 400 m to contain computing costs (Figure 2).

The system design represents a "simplest meaningful case," appropriate for a first exploratory study. It is a regular cylinder with plane upper and lower boundaries, and uniform formation properties throughout the "caprock" and "reservoir" sections, respectively (see Table 1). There is no permeability contrast between horizontal and vertical directions. Mass and heat flow across the vertical boundaries is assumed to be negligible.

The grid consists of 30 elements with 49 interfaces (Figure 2). One additional element and 5 interfaces are needed to realize the surface boundary condition. The spacing is uniform with 400 m vertical and 1000 m horizontal distance.

The simulation was extended over a physical time of 94,232 years, requiring 2775 time steps and a total CPU time of approximately 1,500 sec on a CDC 7600 computer. The calculations were made with the simulator SHAFT79, developed at LBL, which features an accurate representation of the thermophysical properties of water substance.

Evolution History

The convection system goes through a series of quite different and distinct evolution patterns before, after about 90,000 years, it reaches a steady state. Interesting mechanisms with positive and negative feedback occur on different time scales. Table 2 summarizes the main evolutionary phases, while figures 3-5 present some illustrative data. In the subsequent discussion, we shall refer to the various reservoir regions by means of grid block names as shown in Figure 2.

The system starts out in gravitational equilibrium (no mass flows), with a typical "natural" temperature gradient of .04 $^{o}C/m$ (see Table 1). The temperature gradient gives rise to a vertical heat flow of .084 W/m^2, corresponding to 2.0 HFU. The total rate of heat loss through the ground surface is 6.6 MW, so that heat injection at the bottom at a rate of 98.2 MW gives rise to net energy gain at a rate of 91.6 MW (see Figure 3). The system starts to heat up at the bottom, center (elements R5 and S5). This process is accompanied by thermal expansion of the pore water and pressure increase. Subsequently water begins to flow upward and outward, and discharge is initiated near the center. Upflow in the center and the heating and accompanying reduction in density of the central water column slow the pressure increase in R5, S5, and after 32 years pressures start to decrease above the heat source. This causes water to flow towards the center at the bottom, which spreads the pressure decline outward and initiates downflow near the periphery. Gradually the mass flow pattern changes from upward

and outward into a toroidal type of configuration, where fluid flows up near the center, flows outward in the shallower portions of the system, downward near the margins, and towards the center near the bottom. After about 200 years pressures start to decrease at the margins below the surface. Mass discharge therefore diminishes near the margins, while it continues to increase near the center. This gives rise to the pronounced peak in net mass discharge after 280 years (see Figure 3). After about 700 years recharge begins at the margins. As time goes on, the convective flow rates increase (Figure 4), and the pattern expands towards the margins to establish a coherent motion throughout the reservoir. The steep increase in convection rates in the period from 300 - 1000 years is caused by a positive feedback process: upflow of hot water in the center begins to heat up shallower portions of the reservoir (see the increase in temperature of R1 after 600 years, Figure 5), thereby reducing the viscosity of the flowing water and increasing convection rates. Convection rates become so large that the temperatures immediately above the heat source start to decline, due to large inflow of colder waters (see the temperature maximum for R5 after 600 years). This process counteracts the preceding increase in convection rates, and stabilizes flows at somewhat smaller values after about 2000 years (Figure 4). Temperatures below the surface start increasing after 1000 years (element C1, Figure 5), slowly increasing conductive heat loss and decreasing the net rate of energy gain. Subsequently the system goes through a long period characterized by a slow increase in temperatures throughout, while minor rearrangements in convection patterns continue to take place. The latter is illustrated by the changes in flow direction between S3/R3 and T2/T3 (Figure 4). The particular way in which these changes occur is obviously dependent upon the spatial discretization employed in the simulation. It is likely that some of the non-linear feedback processes mentioned above are also affected (exaggerated) by discretization effects. No significant event occurs until, after 39,000 years, boiling commences in element R1. This gives rise to a number of important changes. Steam saturation in R1 increases fairly rapidly, reaching 10% after 40,000 years, and 15% after 46,000 years. After the transition to two-phase conditions, temperatures and hence pressures remain practically constant in the two-phase zone (see Figure 5), additional heat inflow being absorbed by boiling. Pressures continue to decline in the single-phase regions, due to heating up and reduction in density with increasing temperature. Thus the pressure gradients which drive flow towards the two-phase zone diminish. The consequences can be read from Figure 4: the upflow near the center diminishes rapidly (R2/R3), and the hot upwelling waters are diverted outward in a funnel-like pattern (cf. the steep increase in flow rates for S3/R3 and T2/T3 as examples). This outward diversion of upwelling hot waters is the main mechanism by which the boiling spreads laterally. A

minor contribution to the spreading comes from horizontal outward flow of water. The latter is inhibited by permeability reduction for water flow due to buildup of steam saturation. Relative permeability for water is reduced to 40% and 24%, respectively, for steam saturations of 10% and 15%. Horizontal steam flow remains small at all times, and does not contribute significantly to the lateral spreading of boiling. Subsequent phase transitions occur in S1 (after 43,500 years), T1 (after 46,000 years), and U1 (after 49,000 years). Temperatures and pressures remain essentially constant in the two-phase zones. Therefore, pressures do not change much in the caprock overlying the two-phase zones, so that mass discharge remains approximately constant. However, pressures continue to decline at the margins, causing recharge rates to increase and giving rise to the sharp drop in net rate of mass loss after 50,000 years (Figure 3). Several additional phase transitions occur (elements R2, S2, C1) until, after about 90,000 years, the system approaches a steady state.

The Steady State

As the rate of surface heat loss approaches the rate at which energy is injected at the base, and as the rate of mass recharge approaches the rate of discharge, the net rates of energy gain and mass loss go to zero (Figure 3). In the steady state all flow patterns are stationary (time-independent), and mass- and energy-content of the system remains constant. Table 3 presents data on the rates of mass and energy flow through the ground surface after 92,979 years. The rate of energy discharge is to within 0.1% of the injected energy. (A more accurate steady state could be obtained using a finer mesh.) The energy discharge is approximately 90% conductive and 10% convective, with energy flux largest above the heat source, as expected. Fluid discharge is also strongest above the heat source. It tapers off away from the center, and changes into recharge towards the margins. In the steady state, the system has lost 21.6% of its initial mass content, but its energy content has increased 3.2 times. Of the heat injected in 92,979 years, only 27.2% remains in the system, the rest having been discharged to the atmosphere.

Conclusions

This work demonstrates the application of numerical simulation methods to study the natural evolution of vapor-dominated geothermal reservoirs. However, the large computational effort involved in this presently limits obtainable spatial resolution and accuracy of results.

The numerical simulation reveals several mechanisms, which are operative at different stages in the evolution of the system. The more important mechanisms are: (1) initiation of intense reservoir-wide convection by means of a positive feedback between convective heat transport and reduction in fluid viscosity, and (2) the lateral spreading of boiling by means of displacement of upward convection away from two-phase zones.

Although only a relatively thin vapor-dominated zone was produced in these calculations, the steady state results demonstrate many of the features inferred from the study of natural systems, including: 1) vertical counterflow of steam and liquid water with steam rising and condensate falling; 2) lateral movement of steam from the center toward the edges of the system; 3) condensation of steam due to upward conductive heat loss with condensate draining downwards to a liquid dominated zone where it flows toward a central zone of boiling; 4) an interface between a shallow, liquid saturated zone and the vapor-dominated zone that is at a temperature near the enthalpy maximum of saturated steam (236 ^{o}C); 5) boiling in the central part of the underlying liquid dominated zone with boiling rates increasing with depth to a maximum close to the bottom of the two-phase zone.

It is to be emphasized that the present study was made for a rather schematic reservoir model, and more realistic features will be incorporated in future simulations.

References

1. James, R., Wairakei and Larderello: Geothermal Power Systems Compared, N.Z. J. Sci. 11, 1968, 706-771.

2. Sestini, G., Superheating of Geothermal Steam, Geothermics, 1970, special issue 2, 622-648.

3. White, D.E., Muffler, L.J.P., and Truesdell, A.H., Vapor-Dominated Hydrothermal Systems Compared with Hot-Water Systems, Econ. Geol., vol. 66(1), 1971, 75-97.

4. Truesdell, A.H., and White, D.E., Production of Superheated Steam from Vapor-Dominated Geothermal Reservoirs, Geothermics, 1973, vol. 2, nos. 3-4, 154-173.

5. D'Amore, F., and Truesdell, A.H., Models for Steam Chemistry at Larderello and The Geysers, in Proceedings Fifth Workshop Geothermal Reservoir Engineering, Stanford, California, 1979, 283-297.

6. Witherspoon, P.A., Neumann, S.P., Sorey, M.L., and Lippmann, M.J., Modeling Geothermal Systems, Lawrence Berkeley Laboratory Report LBL-3263, Berkeley, California, May 1975.

7. Coats, K.H., Ramesh, A.B., and Winestock, A.G., Numerical Modeling of Thermal Reservoir Behavior, in Oil Sands, 1977, 399-410.

8. Sheu, J.P., Torrance, K.E., and Turcotte, D.L., On the Structure of Two-Phase Hydrothermal Flows in Permeable Media, J. of Geoph. Res., vol. 84, no. B13, 1979, 7524-7532.

TABLE 1: RESERVOIR PARAMETERS

GEOMETRY

Cylinder with 2.4 km height, 5 km radius

FORMATION PARAMETERS

	CAPROCK (top 400 m)	RESERVOIR (bottom 2000 m)
density	2600 kg/m^3	2600 kg/m^3
porosity	.10	.10
permeability	$.3 \times 10^{-15}$ m^2	100×10^{-15} m^2
specific heat	775 J/kg ^oC	775 J/kg ^oC
heat conductivity	2.1 W/m ^oC	2.1 W/m ^oC

(no compressibility or thermal expansivity)

Corey relative permeability functions with $k_{rw} = .5$, $k_{rs} = 0$

BOUNDARY CONDITIONS

top: average ambient ground surface conditions of
$T = 10\ ^oC$, $p = 10^5$ Pa ($\hat{=}$ 1 bar)

mantle: "no flow"

bottom: over circle with 2 km radius at center have heat flow of 7.8125 W/m^2 (corresponding to an average heat flow of 1.25 W/m^2 over the entire bottom area); otherwise "no flow"

INITIAL CONDITIONS

temperature gradient $|\nabla T| = .04\ ^oC/m$ (i.e., "natural" heat flow of .084 $W/m^2 \hat{=}$ 2.0 HFU)

pressure gradient is hydrostatic (gravitational equilibrium with no mass flow)

TABLE 2: EVOLUTION OF A VAPOR-DOMINATED HYDROTHERMAL SYSTEM

PHASE	HEAT EFFECTS	FLUID FLOW
initial state	"natural" heat flow	no mass flow (gravitational equilibrium with surface waters)
"dormant" state (0-300 years)	temperature rises above heat source	slow mass flow away from heat source (thermal expansion)
evolution of intense convection above heat source (300-1,000 years)	rapid increase in temperatures upward from heat source	rapid increase in mass flow (positive feedback from temperature-dependence of viscosity)
evolution of reservoir-wide convection (1,000-39,000 years)	spreading of elevated temperatures throughout system	slowly rearranging "toroidal" flow pattern
evolution of boiling (39,000-90,000 years)	stabilization of temperatures (hence pressures) in two-phase zones	"funnel-like" displacement of convective upflow away from two-phase zones, with lateral spreading of boiling
steady state (after 90,000 years)	surface heat loss equals base heat inflow	recharge equals discharge

TABLE 3: Surface Heat Flow and Fluid Discharge and Recharge in Steady State.

Element	Distance from Center (km)	Surface Area (km^2)	Mass Flux[a] ($kg/sec \cdot km^2$)	Energy Flux[b] (MW/km^2)	Total Mass Flow (kg/sec)	Total Energy[b] Flow (MW)
C1	.5	3.142	1.082	3.018	3.40	9.48
C2	1.5	9.425	.7820	2.371	7.37	22.35
C3	2.5	15.71	.0700	1.348	1.10	21.18
C4	3.5	21.99	-.1251	1.096	-2.75	24.11
C5	4.5	28.27	-.3250	.7417	-9.19	20.97
Entire Surface		78.54			-0.07	98.09

a) Positive for discharge, negative for recharge.

b) Contains conduction and convection.

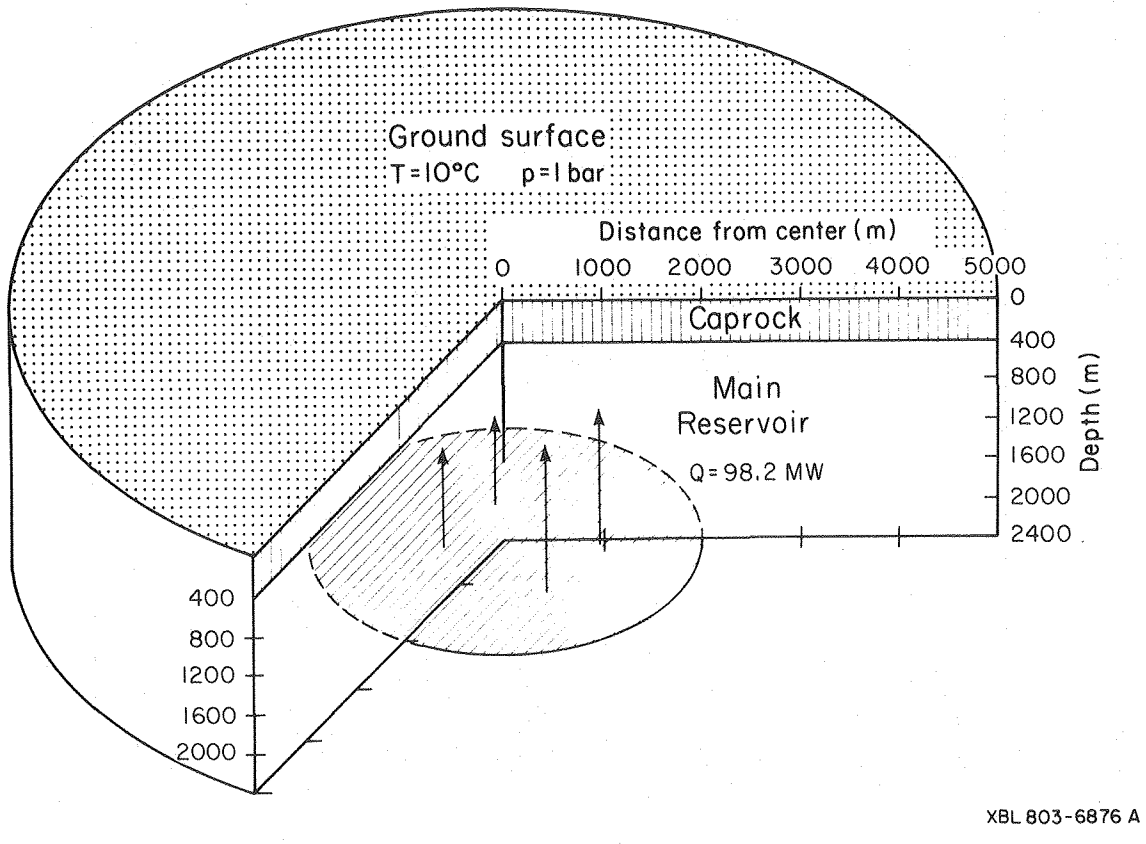

Figure 1. Model of Natural Hydrothermal Convection System (NHCS).

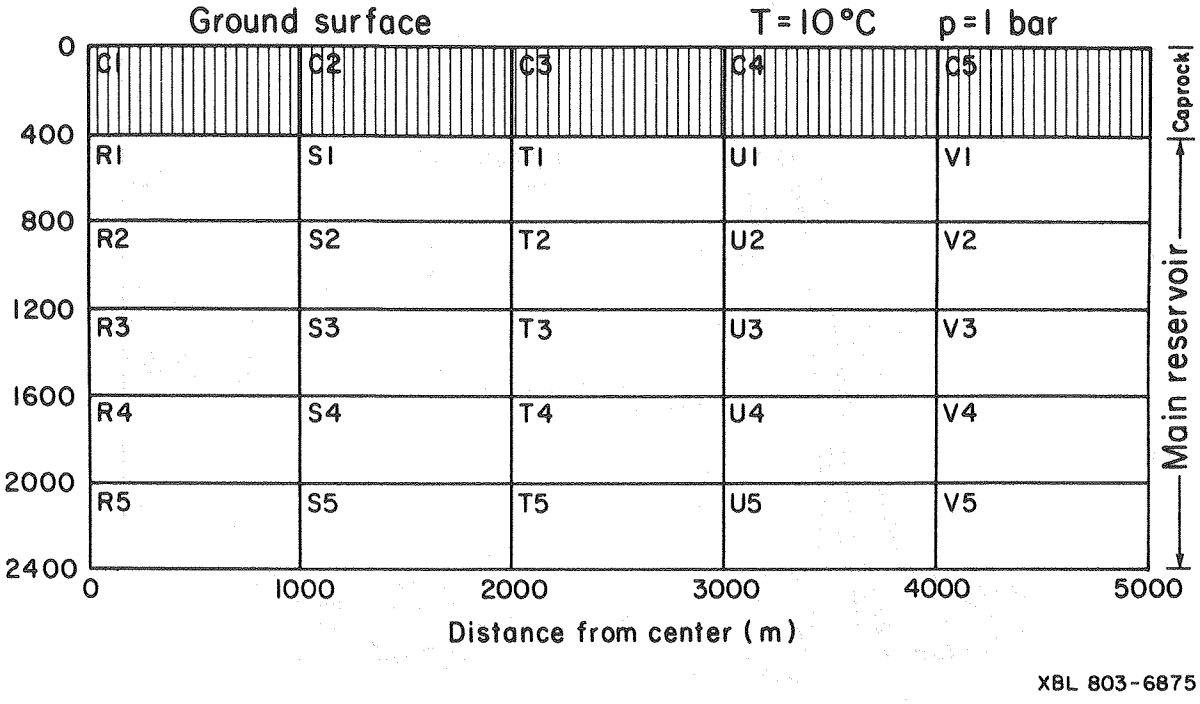

Figure 2. Vertical Cross Section of NHCS. The center line is on the left, and the space discretization with element names is shown.

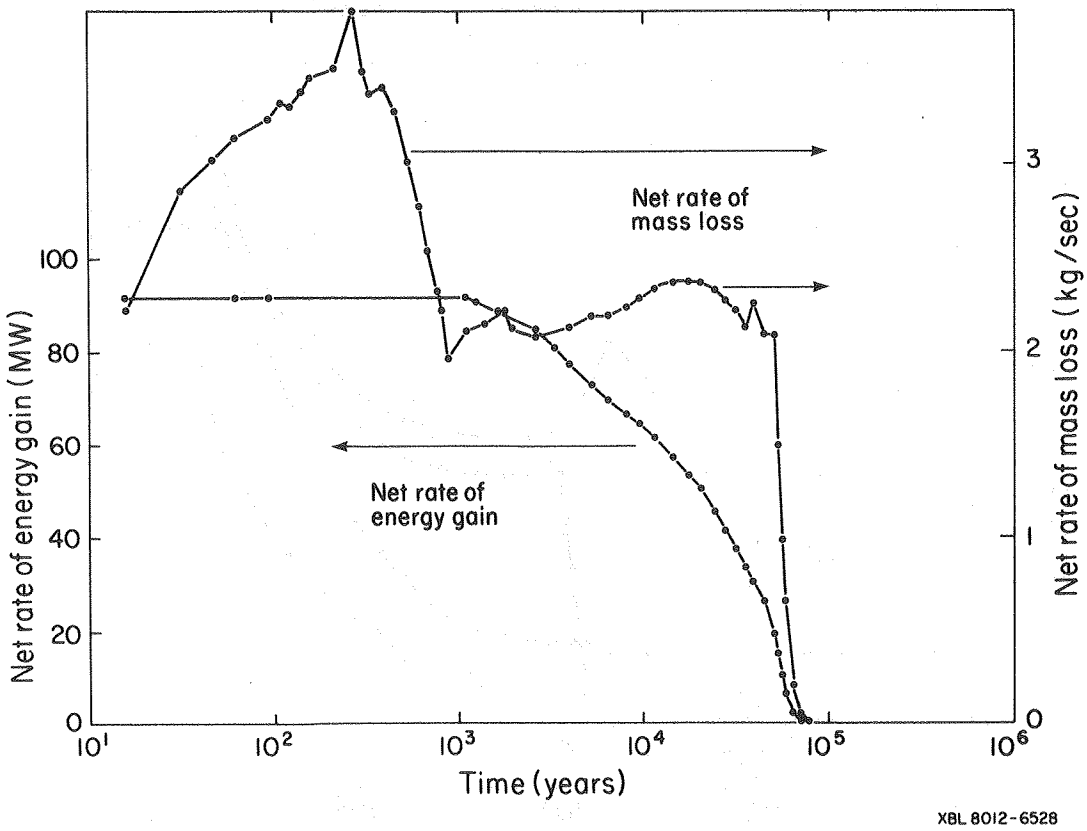

Figure 3. Energy Gain and Mass Loss for NHCS.

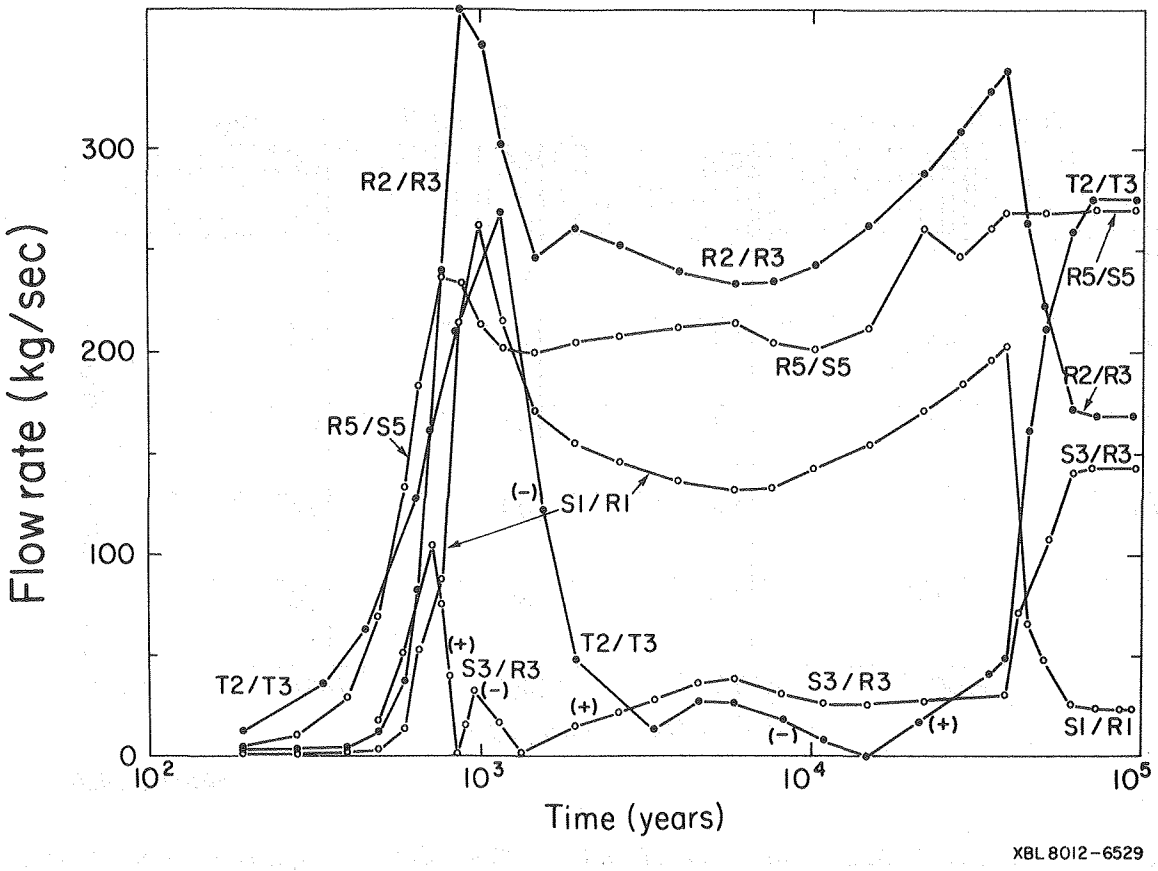

Figure 4. Mass Flow Rates in NHCS. The curves are labeled with the elements between which the flow occurs. Flows are from the second element into the first, unless a curve is labeled (-).

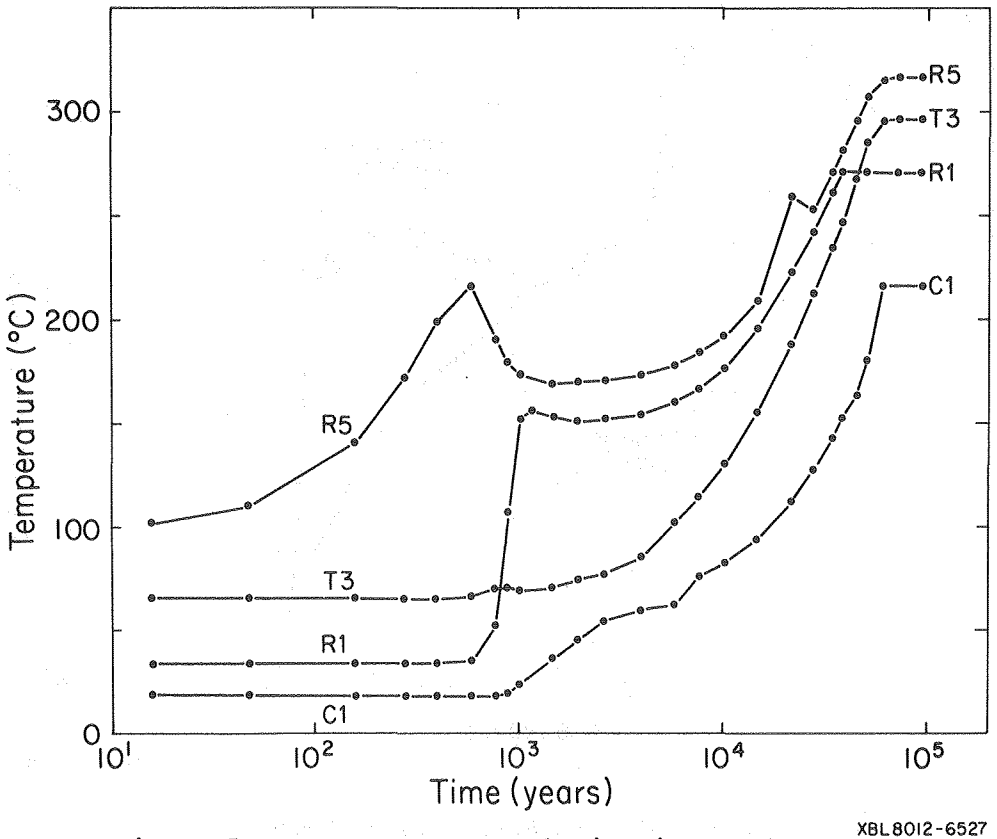

Figure 5. Temperature Evolution in NHCS.